Preprints, 4th IFAC Conference on
Advances in Proportional-Integral-Derivative Control
Almería, Spain | June 12-14, 2024

Bridging Time and Frequency for Low-Order, Model-Based PID Control

M.G. Ortega * **M. Vargas** * **M.G. Satué** * **M.R. Arahal** *
M. Berenguel **

* *Department of Automation and Systems Engineering. University of Seville, Spain. E-mail: {mortega,mvargas,mgarrido16,arahal}@us.es.*
** *Department of Computer Science. University of Almería, Spain. E-mail: beren@ual.es.*

Abstract: In the context of traditional PID model-based control, where sinusoidal or PRBS excitation on a real plant is not advisable or desirable, this paper outlines a method to obtain some relevant information by merely comparing model-based and actual time-domain reaction curves. This comparative analysis yields valuable information that can be subsequently translated into a practical estimate of uncertainty in the frequency domain. This, in turn, will enable the control designer to gain some insight into imposing realistic boundaries for closed-loop response specifications, which will ultimately be consistent with what can be expected from the actual plant response. The conditions for robust stability and robust performance are outlined and further assessed through academic simulation experiments.

Keywords: Process control, linear robust control, system uncertainty, frequency response.

1. INTRODUCTION

Identification based on step time response or reaction curve is extensively used in industrial process control, with the aim of attaining low-order linear models. Obviously, nonlinearities, process variations or high-frequency dynamics are not captured, somehow intentionally, by these models. With respect to the latter, this elementary approach clearly imposes very important limitations in the bandwidth of the model-based control system, as the model will only provide an appropriate description of the system's behavior for a relatively-low frequency range, with moderate or severe uncertainty at higher frequencies (Astrom (1995), Åström and Murray (2021)). These limitations are deemed to be fair payment for the simplicity gained in the subsequent control design.

The basis of classical linear control theory and the core of many well-known textbooks in the field rely on this principle and its inherent trade-off between simplicity and allowed uncertainty (Åström and Hägglund (2006); Skogestad and Postlethwaite (2005); Altmann (2005); Hägglund (2023); Vázquez et al. (2022); Guzmán et al. (2023)).

Frequency response analysis, typically based on sinestream or pseudo-random binary sequence (PRBS) perturbation, on the other hand, provides a simple tool for assessing the accuracy of a given model at a certain frequency range, by comparison of the nominal and experimental frequency responses or by deriving some uncertainty frequency plots. This can be particularly useful when the specifications for the control system are given in, or are translated into, the frequency domain, being the vicinity of the desired crossover frequency the most relevant frequency band.

In many industrial environments, however, the prospect of making a series of experiments that are intended to take the system (or part of it) out of its usual operational routine, leading it into resonance states, may seem unrealistic, unaffordable or downright scary in the eyes of the plant managers and operators. By the same token, the use of more sophisticated techniques in the context of industrial processes, such us evolutionary algorithms for PID tuning based on hyperparameter optimization (Martínez-Luzuriaga and Reynoso-Meza (2023)), is notably challenging, if not nearly unfeasible.

On a different note, even among the control education community, we can witness that, whenever it is time to readjust content in elementary control-related subjects, requiring some sacrifices to be made, frequency-based analysis and design tools can be the easy targets to be kicked out.

Given this state of affairs, if the plain reaction curve is indeed the least we have to settle for, always available as the most immediate, well-known, intuitive and frictionless tool when it comes to experimenting with the system, we can ask ourselves *which additional information can be drawn from it, that enables us to provide simple jet useful guidelines for assessing in the design stage of elementary controllers ?*

This paper tries to answer that question. Given an approximate time-based linear model of the plant under study, this work introduces a simple method that provides a frequency estimation of the underlying multiplicative uncertainty. This is not intended as an exhaustive modelling tool whatsoever. Instead, it has to be understood as a handy tool in assessing the choice of consistent control specifications, saving both, time and effort, while avoiding any attempt of disruptive experimentation on the real plant. On the other hand, in the context of robust control, the specific

design method under consideration can take advantage of this same uncertainty estimation, in order to establish appropriate bounds to ensure closed-loop robustness.

This paper is organized as follows. First, Section 2 outlines some intuitions that can be derived from simple graphical comparison of the modelled and actual reaction curves. Section 3 revisits the classical concepts of additive and multiplicative uncertainties in the frequency domain, while Section 4 exploits this description to establish a convenient link between the information gathered in the time domain and uncertainty described in the frequency domain. Such a link is at the core of the proposed procedure to assist in providing consistent specifications for the controlled system, but this section restricts the study to mere stability conditions. Section 5, on the other hand, deepens this time-frequency connection by additionally tacking robust performance into consideration. Section 6 proposes a typical simulation experiment to test the proposed methodology. Finally, the paper ends offering some conclusions of the work in Section 7.

2. INTUITIONS FROM THE REACTION CURVE

In general, when we exclusively rely on the reaction curve, our intuition suggests the importance of being cautious in specifying how fast we want the resulting closed-loop response to be. It tells us that we should be consistent with the accuracy of our knowledge about the system, given by the apparent discrepancies between modelled and actual step responses.

We can imagine the experimental reaction curve of a particular system, starting from a predefined operation point, given zero initial conditions in their increments. From the response of the actual system, we typically identify a low-order model that captures the most dominant dynamics. Then, we compare the response of the model, $y(t)$, with respect to the response of the actual plant, $y^*(t)$, as illustrated in Fig. 1.

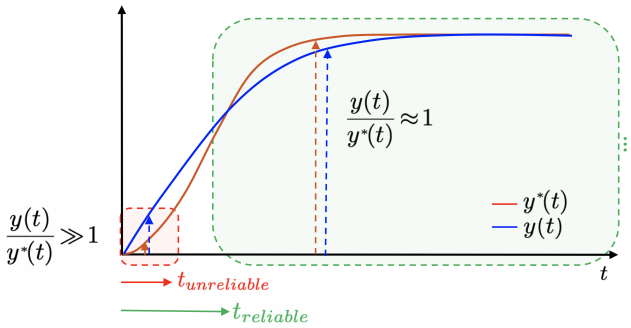

Fig. 1. Example of reaction curve comparison, nominal versus actual plant.

While it is not possible to establish a direct correspondence between a specific time and a particular frequency (Qian and Chen (1999)), we can intuitively infer that, if we specify the desired response time for the controlled system to be close to or longer than the time scale of the identified main dynamics (loosely defined as *reliable time scope*, given by a lower threshold $t_{reliable}$, and highlighted by the green area in Fig. 1), it is expected that we get "acceptable" results. On the contrary, if we specify a comparatively demanding closed-loop performance (corresponding to time scales under the scope of the red area in the figure, coarsely-defined as *unreliable time scope* and given by an upper threshold $t_{unrealiable}$), the results will much likely be unacceptable. Somehow, we can try to rationalize the expected results by arguing that the discrepancy between both incremental signals (actual and nominal responses) around those time scales remain close or become distant from each other, in relative terms, respectively:

$$\frac{y(t)}{y^*(t)} \approx 1 \quad \text{for } t \geq t_{reliable}\,,$$

but

$$\frac{y(t)}{y^*(t)} \gg 1 \quad \text{for } t \leq t_{unrealible}\,.$$

The authors are well aware that this is only an intuitive concept, which may present some loopholes. This is particularly evident when the model exhibits an excess of poles greater than one, leading to a step response with no abrupt change in slope. Similarly, its effectiveness is compromised when applied to systems with dead time.

Therefore, in the next sections, we want to introduce some rigour to these intuitions about what level of uncertainty the designer is facing at different time scales and how to leverage this knowledge to assist in the definition of reliable specifications. Nevertheless, since uncertainties are more effectively addressed in the frequency domain, our focus shifts towards that direction in the upcoming section.

3. ADDITIVE UNCERTAINTY REVISITED

Assuming we are in the context of a SISO system, lets call $G(s)$ the nominal transfer function representing the dynamics of that system (that is our *nominal plant*), while $G^*(s)$ will represent the uncertain, actual description of the system (the *uncertain plant*).

Uncertainty can be described in additive fashion and expressed in the frequency domain Skogestad and Postlethwaite (2005):

$$G^*(j\omega) \;=\; G(j\omega) \;+\; E_a(j\omega) \tag{1}$$

where $E_a(j\omega)$ represents the so-called additive uncertainty, which is typically defined as:

$$E_a(j\omega) \;=\; |W_a(j\omega)|\,\Delta_a(j\omega)\,, \qquad \|\Delta_a\|_\infty \leq 1 \tag{2}$$

where $W_a(j\omega)$ is a weight introduced in order to normalize the uncertainty to be less than 1 in magnitude at every frequency, according to the chosen norm:

$$\|\Delta_a\|_\infty \triangleq \max_\omega |\Delta_a(j\omega)|$$

Usually, the multiplicative formulation for uncertainty is preferred. In this case, the disturbed plant can be said to be:

$$G^*(j\omega) \;=\; G(j\omega)\,(1 + E_m(j\omega)) \tag{3}$$

being $E_m(j\omega)$ the multiplicative uncertainty, defined in a similar way:

$$E_m(j\omega) \;=\; |W_m(j\omega)|\,\Delta_m(j\omega)\,, \qquad \|\Delta_m\|_\infty \leq 1 \tag{4}$$

Clearly, the following relation holds:

$$E_m(j\omega) \;=\; \frac{E_a(j\omega)}{G(j\omega)} \tag{5}$$

Multiplicative uncertainty is more informative, in the sense that, for instance, at frequencies where $|W_m(j\omega)| > 1$, uncertainty exceeds 100% and, evidently, no control based on the nominal model is advisable at those frequencies.

What is described next can be considered one of the main contributions of the paper, namely, a new procedure to theoretically link the time-domain error between the nominal and the actual outputs – which can be easily estimated from simple reaction-curve experiments – to an estimation of the corresponding additive frequency-domain uncertainty.

4. BRIDGING TIME-DOMAIN ERROR AND FREQUENCY-DOMAIN UNCERTAINTY

Considering the time error signal between the actual and the nominal step responses of the system (see Fig.4):

$$e(t) \;=\; y^*(t) - y(t).$$

Assuming U as the step amplitude and applying Laplace transform:

$$e(s) \;=\; y^*(s) - y(s) \;=\; [G^*(s) - G(s)]\,\frac{U}{s}$$
$$s\,e(s) \;=\; U\;[G^*(s) - G(s)]\,,$$

what means that, assuming zero initial conditions, additive uncertainty can be directly obtained from the Laplace transform of the derivative error function:

$$E_a(s) \;=\; \frac{1}{U}\,\mathcal{L}\,[de/dt]\,.$$

Stated in the frequency domain, the Fourier transform of the derivative error signal provides the frequency profile of the additive uncertainty:

$$E_a(j\omega) \;=\; \frac{1}{U}\,\mathcal{F}\,[de/dt]\,.$$

The step-by-step procedure can be described as follows.

- First, we obtain the empirical error signal from both reaction curves:
$$e(t) \;=\; y^*(t) - y(t). \tag{6}$$
- Then, we compute the numerical time derivative of this error signal, preferably scaled by the step amplitude:
$$\dot{e}_{_U}(t) = \frac{1}{U}\,\frac{de(t)}{dt}. \tag{7}$$
- Next, we get the estimation of the additive uncertainty by applying the Fast Fourier Transform (FFT) to the previous signal:
$$\hat{E}_a(j\omega) \;=\; FFT\,[\dot{e}_{_U}(t)]\,. \tag{8}$$
- Finally, by point-to-point division of complex numbers, we get the estimation of the multiplicative uncertainty:
$$\hat{E}_m(j\omega) \;=\; \frac{\hat{E}_a(j\omega)}{G(j\omega)}. \tag{9}$$

This will not provide us with an analytical expression for the multiplicative uncertainty, which, by the way, will not be required. Instead, we just need to evaluate its graphical representation.

The multiplicative uncertainty uses to increase as the frequency does. This fact tells us that, by sticking to our model, we will have absolute lack of knowledge on the behaviour of the actual system at frequencies higher than a cutoff frequency, ω_0, defined as the lowest frequency at which $|\hat{E}_m(j\omega_0)|_{dB} \approx 0$ [dB].

Accordingly, trying to rely on the assumed model to specify, for instance, a cutoff frequency close or over that threshold would most certainly lead to a very poor stability performance on the part of the controlled system. According to this, a consistent specification for the closed-loop step time can be obtained under the condition:

$$t_r^{cl} \gtrsim \frac{\pi}{2\,\omega_0}, \tag{10}$$

where t_r^{cl} stands for the closed-loop rise time, designed in a model-based control synthesis.

The aim of this condition is to guarantee that the resulting closed-loop system has, at least, a stable response. Consequently, we can understand it as a *robust stability* condition. The next section tries to go a step further by focusing on *robust performance*, instead.

5. PROVIDING ROBUST PERFORMANCE

In the previous section, robust stability has been addressed, offering a knowledgeable response for the specification of the closed-loop response time. Now it is time to tackle robust performance, so as to provide additional guidelines with the aim of guaranteeing that the resulting controller, designed using the plant model and the uncertainty estimation, provides much more than just nominal performance.

In this section, we delve into estimating the minimum closed-loop rise times to ensure a certain level of robust performance. This entails achieving a real controlled system behavior that is relatively similar to that obtained on the model.

The approach will rely on the estimation of the maximum expected phase loss at a given frequency, described as a function of the uncertainty associated with that frequency.

Assuming that robust stability has been guaranteed, and, therefore $|W_a(j\omega)| < |G(j\omega)|$ at the frequencies at which the system is being controlled, we are concerned about the maximum phase shift, ϕ_{max}, that the real system can incur with respect to the model at a particular frequency, ω, as a function of the additive uncertainty, $W_a(j\omega)$, associated with that frequency:

$$\angle G^*(j\omega) \geq \angle G(j\omega) - \phi_{max}(\omega) \tag{11}$$

In Figure 2, we illustrate this concept by depicting the Nyquist diagram of an example $G(s)$. For any particular frequency, ω_1, if we assume to know $|W_a(j\omega_1)|$, we can outline the circumference within which $G^*(j\omega_1)$ must lie (shown in red in the figure). Then, we can verify that the maximum possible phase shift that $G^*(j\omega_1)$ can incur

with respect to $G(j\omega_1)$ is the angular separation between $G(j\omega_1)$ and any of the two segments that are tangent to the mentioned circumference, starting from the origin. From this, we can easily derive the following relation:

$$\sin(\phi_{max}(\omega)) = \frac{|W_a(j\omega)|}{|G(j\omega)|} = \frac{|W_m(j\omega)G(j\omega)|}{|G(j\omega)|},$$

leading us to a very convenient expression:

$$\sin(\phi_{max}(\omega)) = |W_m(j\omega)|\,. \tag{12}$$

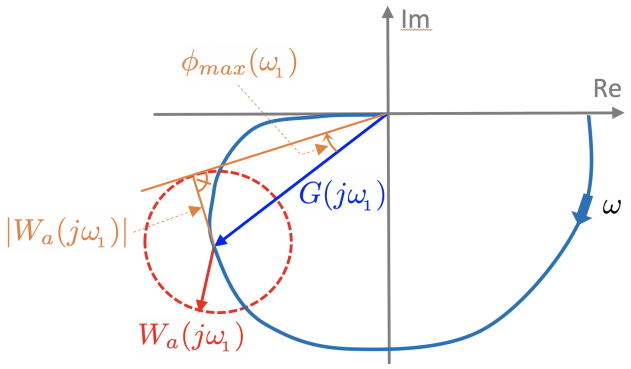

Fig. 2. Estimation of maximum phase loss at a given frequency, ω_1, depending on the additive uncertainty at that frequency.

Figure 3 represents this dependence of the maximum phase loss at a given frequency, $(-\phi_{max}(\omega))$ with the multiplicative uncertainty magnitude expressed in $[dB]$. The maximum phase loss will reach -90^o if $|W_m(j\omega)|_{dB}$ eventually hits $0\,[dB]$. In the plot, however, only a reasonable extent of the variables has been covered.

The level of robust performance is being understood as the worst-case reduction in a nominally designed phase margin. Let us suppose we have, indeed, a controller $C(s)$, providing nominal performance on $G(s)$, according to the designed nominal phase margin. The value of ϕ_{max} can be thought of as the maximum reduction in that theoretical value of the phase margin, provided that the crossover frequency, ω_c, remains roughly the same. So, we are specifically interested in $\phi_{max}(\omega_c)$.

Assuming the controller has been nominally designed with an ample phase margin, let's consider, for instance, approximately 90^o, it might be admissible for this margin to be reduced -15^o or -20^o, without expecting significant deviations in the resulting response. Accordingly, we can use this plot to deduce that a reasonable upper limit for multiplicative uncertainty around the crossover frequency would be in the order of $-10dB$ (please, notice the highlighted red dot on the curve).

Consequently, denoting ω_{10} as the frequency at which $|\hat{E}_m(j\omega_{10})|_{dB} \approx -10\ dB$, *robust performance* can be achieved by fulfilling the following condition [1]:

$$t_r^{cl} \gtrsim \frac{\pi}{\omega_{10}}\,. \tag{13}$$

Finally, it should be emphasized once more that the method relies on the assumption that the gain of the real

[1] Please, notice that, according to this expression, t_r^{cl} is not obtained by dividing by 2, since a phase margin greater than 70^o is assumed.

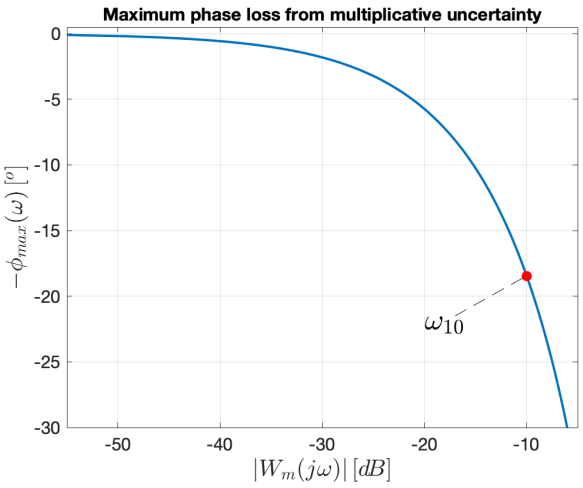

Fig. 3. Representation of the maximum phase loss from the multiplicative uncertainty magnitude.

system is very close to that of the model at the critical frequencies. This hypothesis can be considered realistic, as long as the multiplicative uncertainty is indeed low at these frequencies. For instance, according to the previously exemplified values, the maximum gain variation would be about 30% (associated to a value of $-10\,[dB]$). Notice, however, that this maximum gain variation occurs under alignment of $W_a(j\omega_1)$ with respect to $G(j\omega_1)$ (see Fig. 2), in which case the value of ϕ_{max} would be zero. In contrast, for the value $\phi_{max}(\omega_1)$ estimated in that figure, the gain reduction would be given by the $\cos(\phi_{max}(\omega_1))$, which, for $\phi_{max}(\omega_1) = 20^o$, can be estimated close to 6%.

6. SIMULATION EXPERIMENT

Following a simulated experiment, we will verify that the estimation on the additive and multiplicative uncertainties by means of the algorithm introduced in Section 4 are, in fact, very good estimations of the real ones.

Fig. 4 shows a typical example of nominal versus actual step responses in a typical overdamped system. The error between these two outputs and its time derivative are also provided. The simulated nominal and real [2] plants used for this experiment are specifically the following:

$$G(s) = \frac{10}{(s+1)}\,, \tag{14}$$

$$G^*(s) = \frac{11}{(0.5s+1)\,(0.4s+1)\,(0.1s+1)} \tag{15}$$

where we can see that there is uncertainty, not only in the identified dynamics, but also in the static gain.

First, taking advantage of the priviledged knowledge granted by the theeoretical exercise, we obtain the very additive and multiplicative uncertainties we are trying to estimate by our algorithm. These will derived as follows:

$$E_a(j\omega) = G^*(j\omega) - G(j\omega)$$

$$E_m(j\omega) = \frac{E_a(j\omega)}{G(j\omega)}$$

[2] The real plant is provided for the case the reader would like to reproduce the experiments.

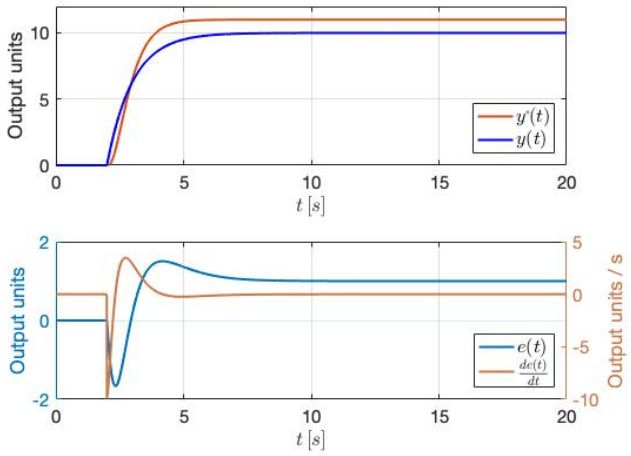

Fig. 4. Nominal versus actual plant experiment, showing typical overdamped step responses, along with the error and its time derivative.

The time responses will be sampled at ten milliseconds interval, $T_m = 0.01\,[s]$, being the corresponding Nyquist frequency $\omega_N = 314.16\,[rad/s]$. Then, we obtain the estimation of these uncertainties $\hat{E}_a(j\omega)$ and $\hat{E}_m(j\omega)$ by means of the proposed algorithm, using (6)-(9). Figure 5 shows the comparison between the actual and estimated additive uncertainties. In the case of the multiplicative uncertainty, though, we are essentially concerned about its magnitude, the comparative evaluation of which is shown in Figure 6, for the case at hand. We can verify that the estimations are quite close to the actual uncertainties up to frequencies close to the Nyquist frequency.

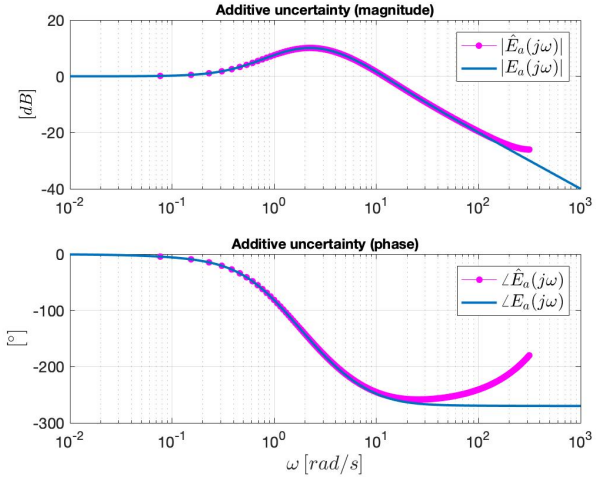

Fig. 5. Comparison between the actual and estimated additive uncertainty for the case study.

Fig. 6 gives us the key insights. From this figure, we can obtain values for $\omega_0 \approx 3\,[rad/s]$ and $\omega_{10} \approx 1\,[rad/s]$. From $\omega \approx 3\,[rad/s]$ on, the multiplicative uncertainty is compromising the stability of the real plant. According to our robust stability threshold, given by (10), we can impose the specification constraint: $t_r^{cl} \gtrsim 0.5\,[s]$. However, if robust performance is also required, the specification

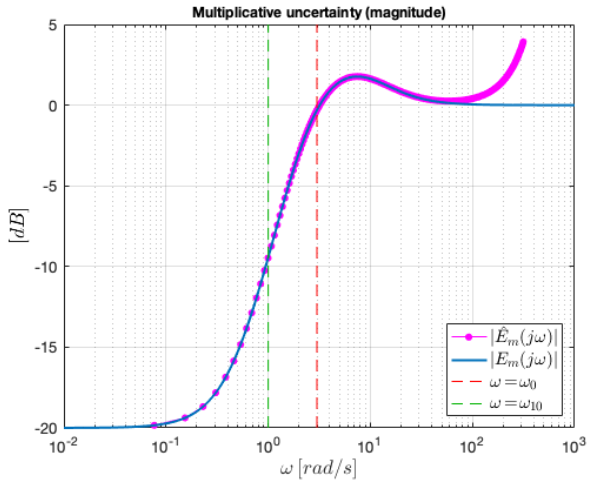

Fig. 6. Comparison between the magnitude of the actual and estimated multiplicative uncertainties for the case study. The relevant frequencies for robust stability and performance are also shown.

constraint: $t_r^{cl} \gtrsim 3\,[s]$, must be imposed instead, according to (13).

To corroborate the hypotheses, let us suppose a model-based controller has been designed by cancelling the dynamics of the model, in the following form:

$$C(s) = \frac{K_c}{s}\frac{1}{G(s)} = \frac{K_c}{s}\frac{s+1}{10}\,. \tag{16}$$

By using this PID controller, (being $T_I = 1\,[s]$, $T_D = 0\,[s]$, and $K_P = \frac{K_c}{10}T_I$), the theoretical closed-loop transfer function from the reference to the output (i.e. the complementary sensitivity transfer function) can be computed as:

$$T(s) = \frac{C(s)G(s)}{1 + C(s)G(s)} = \frac{1}{\frac{1}{K_c}s + 1}\,. \tag{17}$$

Due to the fact that the model-based $T(s)$ is a first-order transfer function, t_r^{cl} can be calculated as:

$$t_r^{cl} = \frac{3}{K_c}\,. \tag{18}$$

In the following figures, nominal versus experimental control results are presented, by specifying different values for the desired closed-loop response time. In all cases, $y^*(t)$ and $y(t)$ represent the actual and model output, respectively, $y^r(t)$ represents the provided reference, while $u^*(t)$ and $u(t)$ refer to the real and model control outputs that are fed into the respective systems. In the experiment shown in Figure 7, K_c has been adjusted for a nominal $t_r^{cl} \approx 3[s]$, the minimum estimated value for achieving robust performance. It can be seen that the actual response is similar to the nominal one, in terms of settling time and absence of overshoot. In Figure 8, on the other hand, K_c has been tuned to obtain a nominal $t_r^{cl} \approx 0.5[s]$, the minimum estimated value just to ensure robust stability. It can be verified that, despite the real closed-loop system is stable, its output exhibits a high overshoot, around 60%, bordering on instability, which drastically differs from the nominal response. Finally, a value of K_c for getting $t_r^{cl} \approx 0.1[s]$ has been tested. As stated before, since this

value is far under the threshold for robust stability, the actual closed-loop response becomes clearly unstable, as shown in Figure 9.

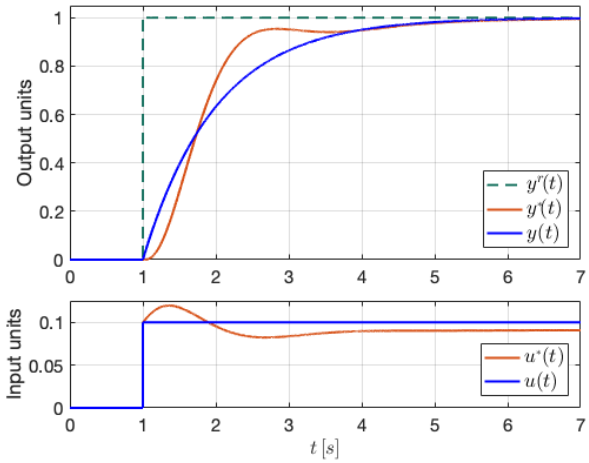

Fig. 7. Nominal vs. actual control results for $t_r^{cl} \approx 3[s]$.

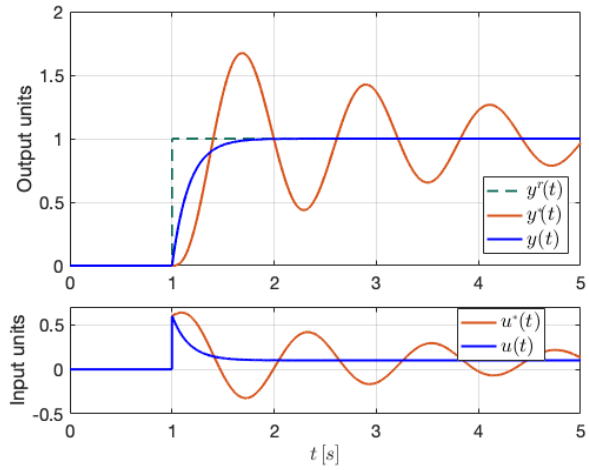

Fig. 8. Nominal vs. actual control results for $t_r^{cl} \approx 0.5[s]$.

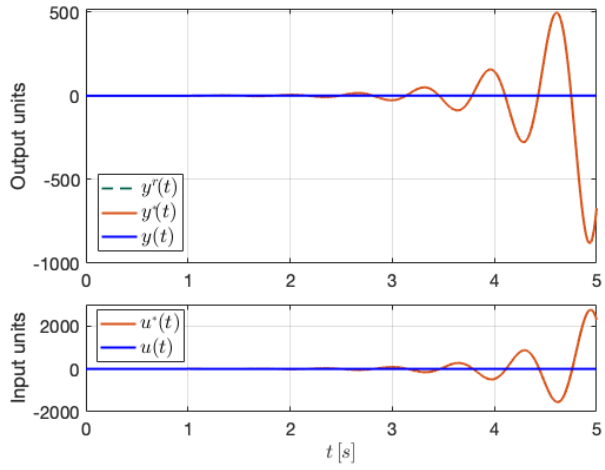

Fig. 9. Nominal vs. actual control results for $t_r^{cl} \approx 0.1[s]$.

7. CONCLUSIONS

This study introduces a valuable connection between the time-domain reaction curve of a dynamic system and the associated additive and multiplicative uncertainties described in the frequency domain. Starting with the step response of the actual system and the corresponding output of a low-order model derived from it, this work describes how the derivative of the error between these two responses can be linked to the frequency-domain uncertainty inherent to the assumption of such a model. Despite the proposed method is clearly rooted in frequency domain concepts, it eventually enables the control designer to formulate consistent control specifications, just by relying on some easy-to-get key measures, readily obtainable from the time domain, without the need of exposing the actual plant to any frequency-based experimentation. These key measures ultimately provide some limits to the closed-loop rise time that should be specified, ensuring robust stability or robust performance as required.

ACKNOWLEDGEMENTS

This work has been carried out within the framework of the project "Optimal Station Control based on Solar Energy with Storage for Electric Vehicle Charging (CONSOLVE)". Grant PID2020-115561RB-C32, funded by MCIN/AEI/10.13039/501100011033 and by ERDF A way of making Europe.

REFERENCES

Altmann, W. (2005). *Practical process control for engineers and technicians*. Elsevier.

Astrom, K.J. (1995). PID controllers: Theory, design and tuning. *Instrument Society of America*.

Åström, K.J. and Hägglund, T. (2006). *Advanced PID Control*. ISA-The Instrumentation, Systems and Automation Society.

Åström, K.J. and Murray, R. (2021). *Feedback systems: an introduction for scientists and engineers*. Princeton university press.

Guzmán, J.L., Costa-Castelló, R., Berenguel, M., and Dormido, S. (2023). *Automatic Control with Interactive Tools*. Springer Nature.

Hägglund, T. (2023). *Process Control in Practice*. Walter de Gruyter GmbH & Co KG.

Martínez-Luzuriaga, P. and Reynoso-Meza, G. (2023). Influence of hyper-parameters in algorithms based on differential evolution for the adjustment of PID-type controllers in SISO processes through mono and multi-objective optimisation. *Revista Iberoamericana de Autom. e Inform. Ind.*, 20(1), 45–55.

Qian, S. and Chen, D. (1999). Joint time-frequency analysis. *IEEE Signal Processing Magazine*, 16(2), 52–67. doi:10.1109/79.752051.

Skogestad, S. and Postlethwaite, I. (2005). *Multivariable Feedback Control: Analysis and Design*. John Wiley & Sons.

Vázquez, U., González Sierra, J., Fernández-Anaya, G., and Hernández-Martínez, E. (2022). Performance analysis of a PID fractional order control in a differential mobile robot. *Revista Iberoamericana de Automática e Informática industrial*, 19(1), 74–83. doi: 10.4995/riai.2021.15036.